Construction and Building Materials 387 (2023) 131655

Contents lists available at ScienceDirect

Construction and Building Materials

journal homepage: www.elsevier.com/locate/conbuildmat

Robust cement composite with low hydration temperature and high mechanical performance achieved by Field's metal and acrylic acid-acrylamide copolymer

Qing Liu [a,b], Xing Ming [b], Jianyu Xu [c], Dongshuai Hou [d], Guoxing Sun [b], Zongjin Li [e,*], Guoqing Geng [a,*]

[a] Department of Civil and Environmental Engineering, National University of Singapore, 117576, Singapore
[b] Joint Key Laboratory of the Ministry of Education, Institute of Applied Physics and Materials Engineering, University of Macau, Avenida da Universidade, Taipa, Macau SAR 999078, China
[c] College of Ocean Engineering and Energy, Guangdong Ocean University, Zhanjiang, Guangdong, China
[d] College of Civil Engineering, Qingdao University of Technology, Qingdao 266000, China
[e] Faculty of Innovation Engineering, Macau University of Science and Technology, Avenida Wai Long, Taipa, Macau SAR 999078, China

ARTICLE INFO

Keywords:
Field's metal
In situ polymerization
Cement composites
Mechanical strength
Low hydration temperature

ABSTRACT

Concrete as an artificial stone owns the weakness of high brittleness and poor flexural strength, dramatically restricting its potential. Therefore, it is crucial to reduce the brittleness and increase the flexural strength of concrete to prolong its service life. Herein, we developed a cement composite with low hydration temperature and high mechanical strength (especially in flexural strength) by combining Field's metal with *in situ* polymerization of acrylic acid (AA) and acrylamide (AM). A cement composite with compressive and flexural strength increased by 8.2% and 174.2% was achieved by tuning the dosage of Field's metal and AA-AM copolymer. The hydration temperature was significantly reduced with the assistance of Field's metal and AA-AM copolymer, inhibiting the formation of the thermal crack. *In situ* polymerization of AA and AM monomers was responsible for improving the intrinsic toughness of cement hydrates by constructing a polymer-cement network, significantly enhancing flexural strength. The *in situ* polymerized AA-AM copolymer acted as a bridge between Field's metal and the cement matrix, improving their interface and contributing to the increased mechanical strength. The filling effect of Field's metal and AA-AM copolymer refined the pore structure of the composite as well. Overall, our findings may offer a promising strategy for developing more robust, resilient, and sustainable cementitious materials.

1. Introduction

Concrete is the most ubiquitous building material in the world as of yet, and its prevalence consumes a large amount of cement which emits lots of greenhouse gases (CO_2) [1]. Thus, it is pivotal to reduce cement consumption, ameliorate crack resistance and durability of concrete, and extend its service life. Construction waste fines have been recycled to prepare the cementitious materials, which reduces the consumption of cement and achieves sustainable materials with good mechanical performance and improved durability [2,3]. Polymers (water-soluble polymer, polymer latex, and polymer powder) have been employed to enhance cement-based materials due to their unique properties of flexibility, corrosion resistance, and adhesion. The polymer-modified cement composites combine the advantages of both polymers and cement, which exhibit excellent mechanical properties and durability and are usually used in harsh environments [4]. The branched polyacrylic acid (PAA) was introduced to modify the cement mortar, which improved the compressive strength [5]. Incorporating polyacrylamide into cementitious materials significantly enhanced flexural strength while maintaining comparable compressive strength [6,7]. Some studies found that adding styrene–butadiene rubber latex improved the mechanical performance, permeability, and freeze–thaw resistance of cementitious materials [8–12]. However, the conventional method of introducing polymers leads to a low ratio of flexural strength to compressive strength, easy entwinement of polymer chains, and weak interplay of cement and polymer. Recently, a burgeoning approach of *in*

* Corresponding authors.

https://doi.org/10.1016/j.conbuildmat.2023.131655
Received 20 March 2023; Received in revised form 29 April 2023; Accepted 2 May 2023
Available online 10 May 2023

situ polymerization of monomers has been used to enhance the mechanical strength and crack resistance of cementitious materials. This approach increases the ratio of flexural strength to compressive strength, ensures the uniform distribution of polymer chains, and strengthens the interplay between cement and polymer. AM was introduced to cementitious materials by *in situ* polymerization, which significantly improved mechanical strength and durability [13–16]. Cement paste was modified by *in situ* polymerization of AA, and the results showed that both the compressive and flexural strength was enhanced [17,18]. Calcium carbonate cement was improved by *in situ* polymerization of 2-hydroxyethylmethacrylate (HEMA) with a sharp reduction of brittleness [19]. Methyl methacrylate was incorporated into the concrete via *in situ* polymerization, which obtained polymer concrete with outstanding mechanical performances at a temperature of −20 °C [20].

Metals or metal alloys that are liquid at or near room temperature are known as liquid metals [21]. A self-limiting native-oxide 'skin' forms easily on the surface of liquid metals, facilitating sticking to different materials. Hence, low melting liquid metal alloys, such as Ga-based alloy EGaIn and the In–Bi–Sn alloy (Field's metal), have been extensively applied in flexible electronics [22,23], energy storage and conversion devices [24,25], catalysis [26], phase-change materials [27], and microstructure characterization of cementitious materials [28–30]. As an innoxious liquid metal, Field's metal was used to enhance the flexural strength and crack resistance of cement paste [31]. Nevertheless, the application of Field's metal and *in situ* polymerization of monomers in improving the performance of cementitious materials has not been reported. Herein, we combine the Field's metal with *in situ* polymerization of AA and AM to fabricate a cement composite with low hydration temperature and strengthened mechanical strength. Incorporating AA-AM copolymer by *in situ* polymerization not only increases the toughness of the cement matrix but also ameliorates the bonding between Field's metal and cement matrix, resulting in enhanced mechanical strength.

This work mainly focuses on fabricating a mechanically strong cement composite by adding Field's metal and *in situ* polymerization of AA and AM. The fluidity of the cement composite was measured by a mini corn test. Real-time monitoring was conducted to determine the effect of Field's metal and *in situ* polymerization of AA and AM on the hydration temperature of cement. The interface between the cement matrix and Field's metal was characterized by contact angle and scanning electron microscopy (SEM) tests. TGA and MIP were employed to characterize the microstructure of the cement composite. The compressive and flexural strength were measured to assess the effect of Field's metal and AA-AM copolymer on the mechanical performance of cement composites. Our results demonstrate the potential of this novel approach in addressing the challenges associated with the use of concrete as a building material.

2. Materials and methods

2.1. Materials

A commercially Portland cement P·I 52.5, provided by Macau Cement Manufacturing CO., LTD, was employed to prepare the cement composites with a water-cement ratio of 0.4. Table 1 presented the chemical compositions of this cement that were measured by an X-ray fluorescence spectrometer. Table 2 listed the basic properties of the Field's metal provided by the Shenyang Jiabie Trading Company, China. Acrylic acid (AA), acrylamide (AM), sodium hydroxide, ammonium persulfate (APS), and N, N, N′, N′-tetramethyl-ethylenediamine (TEMED), tributyl phosphate are all analytical grade provided by Sinopharm Chemical Reagent Co., Ltd. Deionized water was used to prepare the cement composites.

Table 1
Chemical compositions of cement.

Composition (wt%)	CaO	SiO_2	SO_3	Al_2O_3	Fe_2O_3	MgO	K_2O
Cement	65.52	20.19	4.46	4.32	3.07	1.85	0.58

Table 2
Properties of Field's metal.

Item	Field's metal
Elements	In (51%), Bi (32.5%), Sn (16.5%)
Density	7.88 g/cm^3
Melting Point	60 °C
CTE, linear	22.0 mm/m °C
Hardness	11
Tensile strength	33.4 MPa

2.2. Preparation of the cement composites

The process of fabricating Field's metal particles was the same as our previous work [31], and the morphology and particle size distribution of Field's metal particles were shown in Fig. 1. To prepare the monomer solution, AA was dissolved in the deionized water firstly, and hereafter sodium hydroxide was added to neutralize the AA solution. After the solution cooled down to room temperature, AM was added and stirred until dissolution. The initiator APS was then dissolved into the AA-AM solution, followed by adding catalyst TEMED and stirring for 5 min to obtain the monomer solution. The mole ratio of AM/AA was 10%, and the dosage of APS and TEMED was 1% molar of AA and AM monomers.

1%, 3%, and 5% AA and AM monomers based on the mass of cement were added to determine the optimal dosage of AA-AM copolymer. The Field's metal particles (5% wt. of cement, according to [31]) were mixed evenly with cement powder before adding the monomer solution. Then, the prepared monomer solution was added and mixed for 3 min, during which tributyl phosphate was added to eliminate the air bubbles released from the polymerization of AA and AM. The mix proportion of the cement composites was listed in Table 3. F5 and A3 denoted that the dosages of Field's metal and AA-AM copolymer were 5% and 3%, respectively. A3F5 denoted the cement composite with 5% Field's metal and 3% AA-AM copolymer. The water-to-cement ratio was 0.4 for all the cement composites. The fresh cement composites were poured into plastic molds with a size of 10 mm × 40 mm × 160 mm and 40 mm cubes and placed in a vibration table for 1 min. After 48 h, the samples were demoulded and put in a curing room (temperature 20 ± 1 °C and relative humidity ≥ 95%) for 7 and 28 days. Subsequently, samples were taken out and put in a 60 °C water bath for 12 h, followed by placing the heated specimens in a vacuum oven for 2 h to accelerate the flow of the melted Field's metal in the cement matrix. After that, the samples were conducted with the mechanical strength test.

2.3. Methods

2.3.1. Fluidity

A truncated cone (mini cone) mold with a bottom diameter of 60 mm, a top diameter of 36 mm, and a height of 60 mm was used to measure the fluidity of fresh cement composites based on GB/T 8077–2012. The fresh cement composites were poured into the truncated cone placed on a glass plate and then lifted slowly. The fluidity of the sample was defined as the average value of the maximum spread diameter and its perpendicular diameter.

2.3.2. Hydration temperature

The hydration temperature of cement composites was detected by a data logger equipped with a type K thermal couple [32]. 1 kg of fresh cement composites was poured into a container with the thermal couple in the center. The data were recorded from 0 to 72 h with an interval of 10 s.

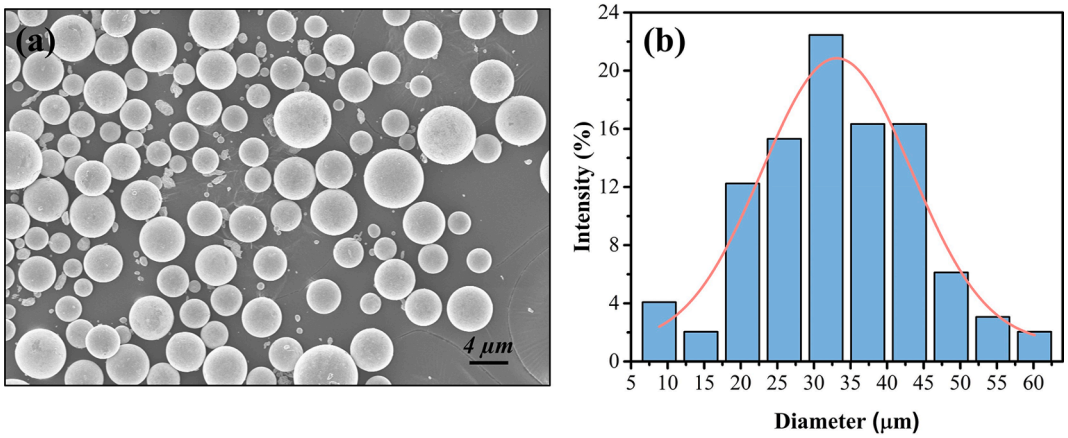

Fig. 1. (a) Morphology of Field's metal particles; (b) Particle size distribution.

Table 3
Mix proportion of cement composites.

MIX ID	Cement/g	Water/g	Field's metal/g	AA-AM monomers/g
RF	100	40	–	–
F5	100	40	5	–
A3	100	40	–	3
A3F5	100	40	5	3

2.3.3. Contact angle

The contact angle of Field's metal was measured by a Contact Angle Meter (SDC-200SS). The Field's metal was melted and cast into a petri dish (diameter: 35 mm; height: 12 mm) to fabricate the disk. After demoulded, one of the disks was immersed into an AA-AM copolymer solution and then taken out to evaporate the water. After that, the disk with and without AA-AM copolymer was conducted to the contact angle measurement using deionized water as a medium. The contact angle was tested at three different locations for each disk to get the average value.

2.3.4. Scanning electron microscopy and optical microscopy

Fragments of samples subjected to compressive strength were collected and immersed in isopropanol to stop the cement hydration. Fragments of samples with AA-AM copolymer and Field's metal were immersed in a 5% HCl solution for 5 min, followed by washing using deionized water, and then the washed samples were dried and stored in a vacuum desiccator. Scanning electron microscopy (SEM) was tested using a Zeiss Zigma FESEM equipped with an energy dispersive spectroscopy. Samples were coated with a thin layer of Pt to increase the conductivity. The accelerating voltage was 5 kV, and the working distance was 4.9 mm.

For the optical microscopy investigations, slices were cut from the cement composite after curing for 28 days and soaked in isopropanol for 1 day. The slices were dried in a vacuum oven and placed in a vacuum desiccator with silica gel to remove the isopropanol. After that, the discs were impregnated with an epoxy resin under vacuum and polished from 10 μm to 0.25 μm with a diamond polishing spray.

2.3.5. Thermalgravimetric analyses

Thermalgravimetric analyses (TGA) were conducted on an instrument SDT-Q600 at a heating rate of 10 °C/min in a nitrogen atmosphere with a temperature range of 30–800 °C.

2.3.6. X-ray diffraction

An X-ray diffractometer (Rigaku Smartlab 9000 W) with CuKα radiation was used to measure the X-ray diffraction (XRD) pattern. The scan range was 5° to 60° with a scan rate of 10°/min under a working voltage of 20 kV and a current of 20 mA.

2.3.7. Mechanical strength test

The compressive strength of samples with a size of 40 mm was measured using a Universal Testing Machine (Instron, 250 kN) with a loading rate of 1 mm/min. Three samples were tested for each mix. The flexural strength of samples (10 mm × 40 mm 160 mm) was measured using an MTS (Exceed E44, 30 kN) with a loading rate of 0.01 mm/s and a span length of 100 mm. Four samples were tested for each mix.

2.3.8. Mercury intrusion porosimetry

The pore structure for each mix was measured using a mercury intrusion porosimetry (MIP) PoreMaster 33 GT with a contact angle of 140°. For MIP, samples subjected to compressive strength were crushed and placed in a plastic bottle filled with isopropanol to terminate the hydration. After 7 days, these samples were taken out and dried in a vacuum oven at 60 °C until reaching constant weight. The dried samples were stored in a vacuum desiccator with silica gel before the MIP test.

3. Results and conclusion

3.1. Optimization of AA-AM copolymer content

The flexural strength of cement pastes with various dosages of AA-AM copolymer is shown in Fig. 2. Increasing the dosage of AA-AM copolymer corresponds to an improvement in flexural strength

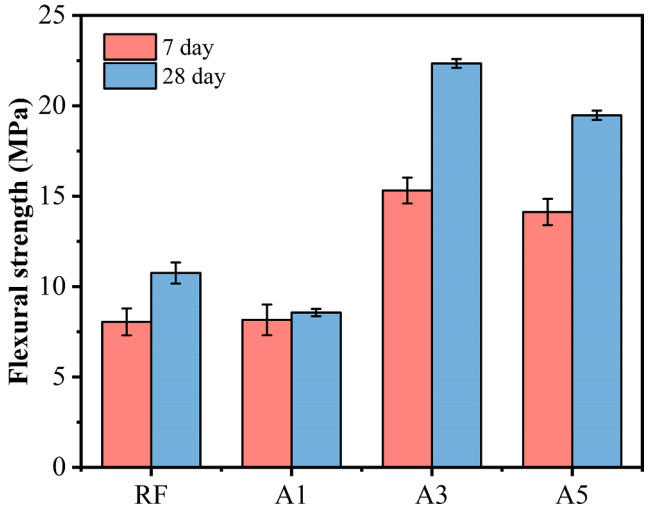

Fig. 2. The flexural strength of cement pastes with different dosages of AA-AM copolymer. A1, A3, and A5 denote that the dosage of AA-AM copolymer is respectively 1%, 3%, and 5%.

regardless of curing time, except for samples with 1% AA-AM copolymer. Samples with 3% AA-AM copolymer exhibit the highest 28-day flexural strength of 22.34 MPa, approximately 107% higher than the reference sample. The decreased flexural strength for samples with 1% AA-AM copolymer is attributed to the poor polymerization of AA and AM that becomes defects in the cement matrix, which has been proved in [33,34]. The interpenetrating polymer network built by *in situ* polymerization of AA and AM in the cement matrix, accompanied by the crosslinking of the polymer network and cement hydrates, is responsible for improving flexural strength. However, further incorporating 5% AA-AM copolymer decreases the flexural strength due to the inherent softness of the polymer, as shown in Fig. 2. Therefore, the optimal dosage of AA-AM copolymer is 3% for the cement paste with a w/c of 0.4, which will be used in the following experiment.

3.2. Fluidity of the cement composites

Fig. 3 depicts the effect of Field's metal and AA-AM copolymer on the fluidity of cement composites. The fluidity of the cement composites is increased with the addition of AA-AM copolymer, while cement composites with only Field's metal are decreased. The increased fluidity for A3 and A3F5 is attributed to the adsorption of AA-AM copolymer on the surface of cement particles, which hinders the aggregation of cement particles. Furthermore, the ball-bearing effect [35] offered by AA-AM copolymer contributes to the increased fluidity. It is noteworthy that A3F5 has a fluidity of 17.75 cm, slightly higher than A3 (17.20 cm). AA-AM copolymer anchors on the Field's metal via a thin 'oxide skin layer' that is generated on its surface [36] or the hydrogen bond between polyvinyl alcohol (PVA) left on the surface of Field's metal particles and AA-AM copolymer [37], which separates them from cement particles, further increasing the fluidity. The Field's metal can absorb water due to the thin PVA film adhering around the particles and its intrinsic hydrophilic (see Fig. 7), decreasing the effective water-cement ratio of cement paste, which is detrimental to the fluidity of the cement composites. Thus, samples with 5% Field's metal have slightly lower fluidity than the reference mixture.

3.3. Temperature evolution of the cement hydration

The temperature evolution of the cement composites with and without Field's metal and AA-AM copolymer is illustrated in Fig. 4(a). The peak temperature of cement hydration is decreased from 65.28 °C for the reference sample to 57.92 °C for those with 5% Field's metal without altering the time to reach it, indicating that adding Field's metal

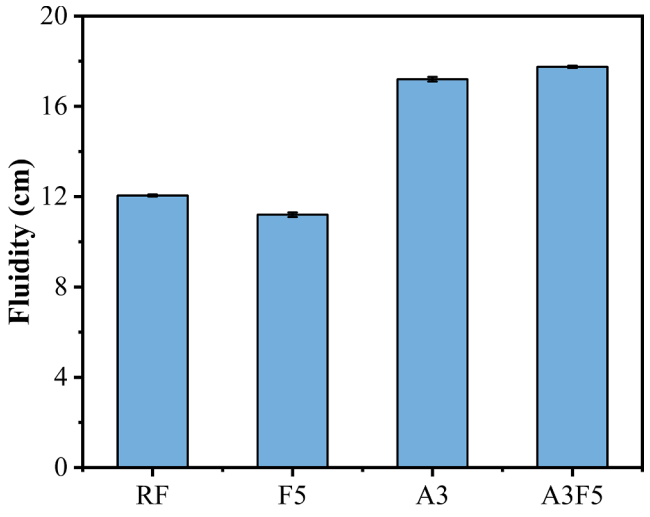

Fig. 3. Effect of Field's metal and AA-AM copolymer on the fluidity of cement composites.

reduces the hydration heat without changing the hydration behavior of cement. Because Field's metal has high volumetric latent heat (315 MJ/m^3), when it transfers from a solid state into a liquid state, it needs to absorb the heat released from cement hydration, resulting in a lower peak temperature. In contrast, incorporating AA-AM copolymer not only postpones the arrival time of peak temperature but also significantly reduces the peak temperature. Although the peak temperature is reduced, the total hydration heat is not changed, which is supported by the finding that the area below the temperature evolution curves for A3 is at the same level as the reference mixture (Fig. 4(b)). This means the cement hydration is retarded and proceeds slowly to restrain the peak temperature. The absorption of AA-AM copolymer on the cement grains limits the dissolution of calcium ions and the nucleation of cement hydrates [38] and thus retards cement hydration. Combining Field's metal and AA-AM copolymer further decreases the peak temperature to 44.41 °C and delays the corresponding time to reach it, resulting from the retardation effect of AA-AM copolymer and the heat absorption of Field's metal. It is worth noting that a peak temperature appears between 0 and 3 h for A3 and A3F5, which is related to the polymerization reaction of AA and AM. The appearance of this peak temperature confirms that the polymerization reaction occurs during the cement hydration.

The area below the temperature evolution curves can be used to describe the heat release of the cement composites. As shown in Fig. 4 (b), cement composites with Field's metal exhibit a lower area in comparison to the reference sample, signifying that the heat release is reduced. The area of A3 and A3F5 is slightly higher than that of RF and F5, respectively, which is attributed to the polymerization of AA and AM that releases heat. The heat release is reduced under the coupling effect of Field's metal and AA-AM copolymer, accompanied by a drastic decrease in the peak temperature, decreasing the thermal stress from cement hydration and thus mitigating the risk of forming thermal cracks. Therefore, Field's metal and *in situ* polymerization of AA and AM can be applied to fabricate cementitious materials with low hydration temperature and high crack resistance.

3.4. Hydration products

The TGA results of cement composites with Field's metal and AA-AM copolymer are presented in Fig. 5. The mass loss between 400 and 500 °C is related to the decomposition of calcium hydroxide (CH), and its peak decomposition temperature shifts to the left, indicating that the stability of the composites is reduced. The mass loss ranges from 50 °C to 200 °C is related to the decomposition of ettringite, monocarbonate, and calcium-silicate-hydrate. It is apparent that only incorporating Field's metal has limited influence on the hydration products of cement. However, samples with AA-AM copolymer have a higher mass loss of carbonated phases (600–800 °C) than samples with and without Field's metal. This phenomenon is inconsistent with the result of [39] carbonation is inhibited by the chelation of calcium ions and superplasticizers. Here, we speculate that the *in situ* polymerized AA-AM copolymer in the cement matrix owns a high capacity for water retention [40], which maintains high humidity to facilitate the dissolution of CO_2 and therefore promotes the carbonation of cement hydrates. The tangential method is employed to calculate the content of CH, and the result is illustrated in Fig. 5(b). Introducing Field's metal and AA-AM copolymer decreases the CH content, with A3 showing the lowest CH content, indicating the retardation effect on cement hydration. The slight decrease of CH content in F5 is ascribed to the reaction of CH with cement hydrates like ettringite [41] after heating. The content of ettringite for A3F5 is lower than that of A3, which is in agreement with previous studies [42,43]. The sharp reduction in CH content for samples with 3% AA-AM copolymer results from the retardation effect of AA-AM copolymer on cement hydration via the strong absorption of the cement particles [44]. Samples with Field's metal and AA-AM copolymer show higher CH content than that with AA-AM copolymer because the

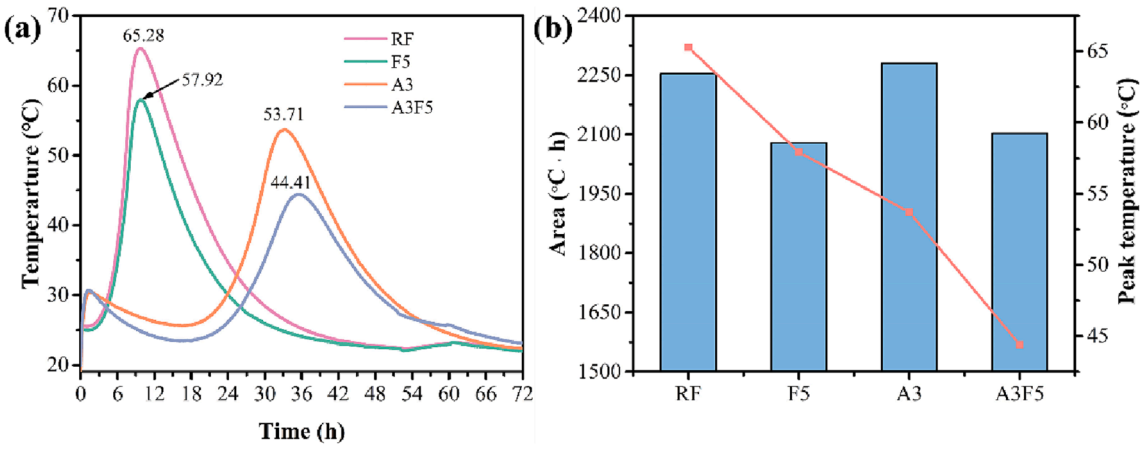

Fig. 4. (a) Temperature evolution of the cement hydration; (b) The area and peak temperature of temperature evolution curves.

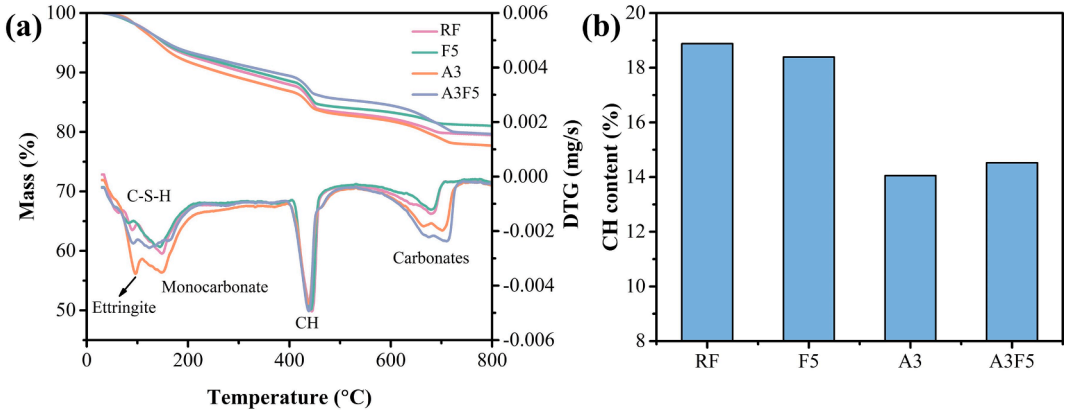

Fig. 5. (a) TGA results of the cement composites after curing for 28 days; (b) Content of calcium hydroxide (CH).

unhydrated cement grains caused by the retardation effect of AA-AM copolymer are accelerated to react under the heating curing and thus produce more CH. Accelerated hydration after heating curing is conducive to the improvement of mechanical strength, as discussed in Section 3.6.

The phase assemblage of cement composites with the addition of Field's metal and AA-AM copolymer is presented in Fig. 6. After heating curing, samples with Field's metal (F5) show a lower intensity in CH in comparison to the reference sample, which is consistent with the TGA results. It is evident that the peak intensity of CH is significantly reduced in the presence of AA-AM copolymer, indicating that cement hydration is inhibited. The adsorption of AA-AM copolymer on the cement grains is responsible for the delayed cement hydration. The delayed cement hydration remains many unhydrated cement grains that are stimulated to rehydration after being subjected to heating, which leads to the increment in the CH of samples with Field's metal and AA-AM copolymer.

3.5. Microstructure

The microstructure of cement composites F5 and A3F5 is shown in Fig. 7. There is a microcrack between the Field's metal particle and cement matrix in F5 (Fig. 7(a)), suggesting that the interfacial transition zone (ITZ) between them is weak. The cracks produced by the external load propagate along this zone quickly, impairing the mechanical strength. For A3F5, the ITZ is dense without microcracks, and the bonding between them is strong (Fig. 7(b)). From the enlarged image of Fig. 7(c) and 7(d), it can be seen that the surface structure of Field's metal in F5 is porous, while that in A3F5 is compact. The dense inner structure is attributed to the filling effect of AA-AM copolymer and the

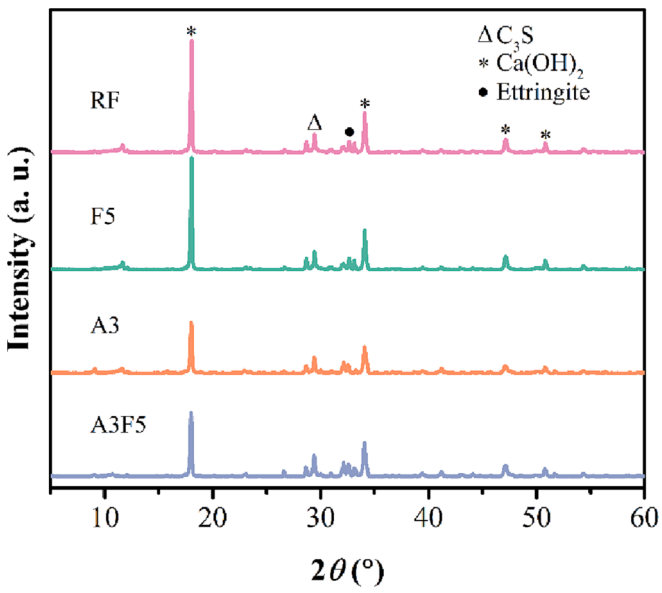

Fig. 6. XRD results of the cement composites after curing for 28 days.

reduction of a water film surrounding the Field's metal caused by the retarded flocculation of cement particles [45] with the assistance of AA-AM copolymer. The contact angle of Field's metal is reduced after being coated with a thin layer of AA-AM copolymer (Fig. 8), suggesting that

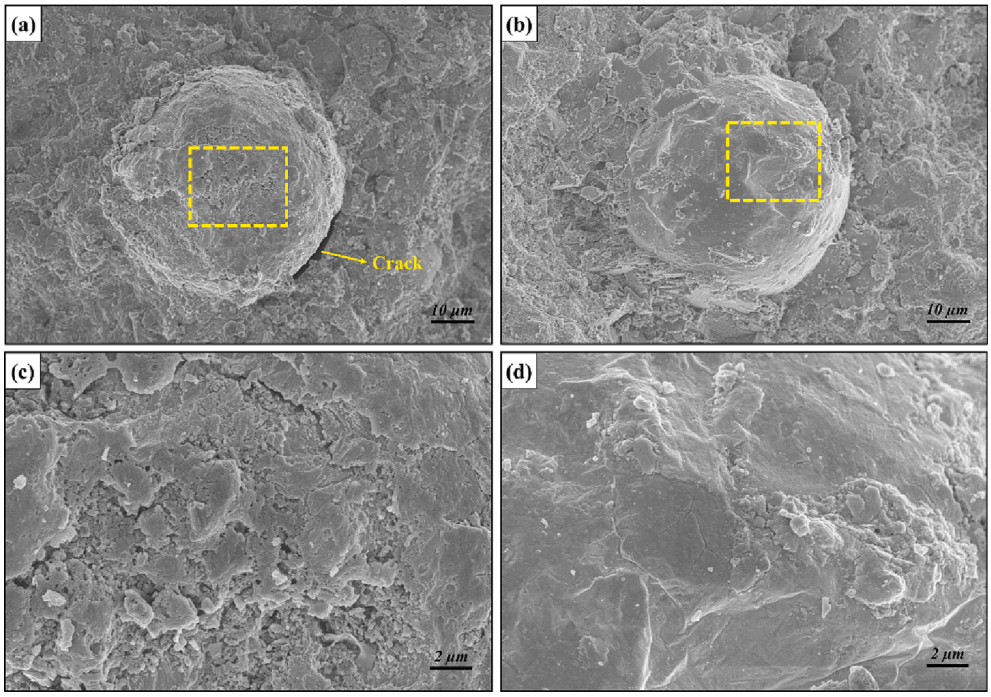

Fig. 7. SEM images of the cement composites. (a) F5; (b) A3F5; (c) and (d) are the zoomed image of yellow dotted rectangles in (a) and (b), respectively. (For interpretation of the references to colour in this figure legend, the reader is referred to the web version of this article.)

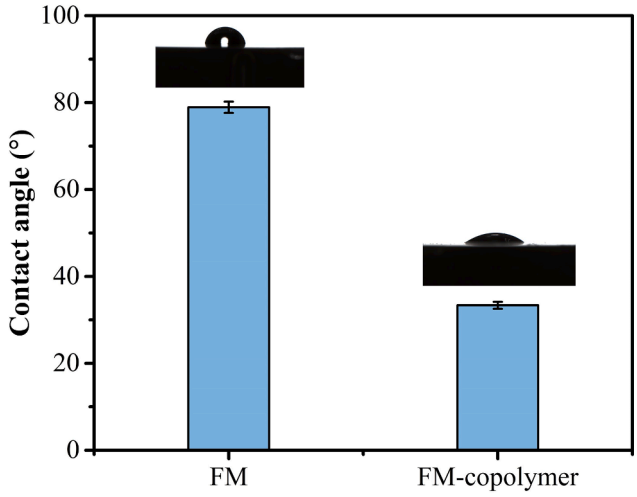

Fig. 8. The contact angle of Field's metal after being coated with a thin layer of AA-AM copolymer. FM denotes Field's metal, and FM-copolymer denotes that Field's metal is coated with a layer of AA-AM copolymer.

AA-AM copolymer improves its hydrophilic and helps cement hydrates to adhere the Field's metal and thus enhances the bonding strength. Furthermore, the high water absorption of AA-AM copolymer restrains the formation of the water film, improving the ITZ. This densified ITZ is beneficial for the improvement of mechanical strength.

Fig. 9 depicts the microstructure of A3F5 after etching in a 5% HCl solution. The polymer network is observed in the cement matrix (Fig. 9 (a)), indicating the occurrence of the polymerization reaction. This polymer network crosslinks with cement hydrates to construct a cement matrix with stiffness and flexibility, which enhances mechanical strength. The connection between the AA-AM copolymer and Field's metal also plays a critical role in improving mechanical strength. As shown in Fig. 9(b), after etching, the cement hydrates and Field's metal are connected by the AA-AM copolymer, which is supported by the EDS result that the main composition of the bridge is the element C. This polymer bridge enhances the bonding strength between cement hydrates and Field's metal, contributing to high mechanical strength. Moreover, AA-AM copolymer connects with cement hydrates via the complexation of carboxyl groups and calcium ions to attach to the Field's metal particles, which constructs a polymer-Field's metal-cement network. This crosslinked network increases the integrity of the cement matrix and provides flexibility to the stiff cement hydrates, improving the mechanical strength by limiting the propagation of microcracks, especially for flexural strength.

Fig. 10 exhibits the morphology of Field's metal particles in the cement matrix. The black circular particles are the Field's metal which distributes casually in the matrix. Molten Field's metal is detected after heating and flows to the adjacent microcracks or space, increasing the contact area with cement hydrates and filling the microcracks. The Field's metal in microcracks imposes a barrier in the route of the load transfer, effectively improving the mechanical strength. Although the fluxion of the molten Field's metal may leave pores on its original site, its flow is constrained (Fig. 10(b)), which imposes little adverse influence on the performance of the cement composite. Field's metal can be used as a phase change material to adjust the indoor temperature due to its low melting point, decreasing the emission of green gases.

3.6. Mechanical performance

The mechanical strength of the cement composites is presented in Fig. 11. The compressive strength is improved with the incorporation of Field's metal and AA-AM copolymer (Fig. 11(a)). Samples with 5% Field's metal show the highest compressive strength of 73.96 MPa at 28 days, approximately 19.6% higher than the reference mixture. The Field's metal melts after heating curing and fills the adjacent microcracks (Fig. 10), restraining the propagation of load along these microcracks and thus enhancing the compressive strength. Additionally, the Field's metal may produce deformation when carrying out the payload, absorbing energy and thus improving the compressive strength. The heating regime also promotes the hydration of unhydrated cement clinkers [46,47], contributing to increased strength. Although

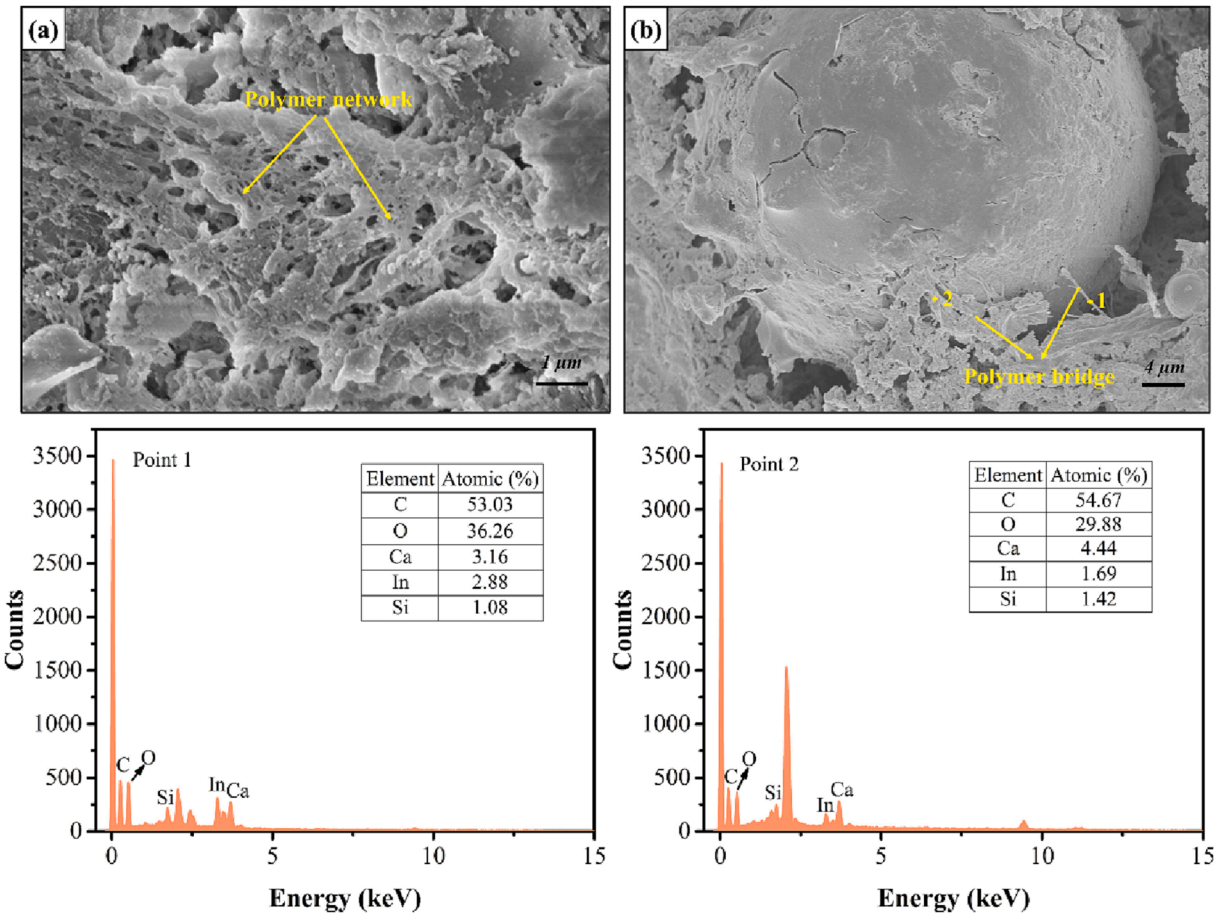

Fig. 9. SEM images and corresponding EDS points of A3F5 after being etched in 5% HCl solution.

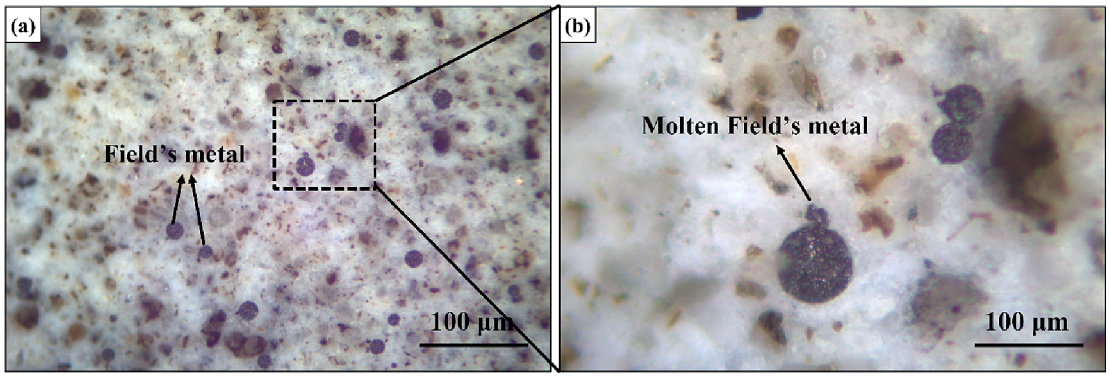

Fig. 10. Optical images of the cement composites with 5% Field's metal after heating.

the compressive strength of samples with AA-AM copolymer (A3 and A3F5) is lower than F5 due to the low stiffness of AA-AM copolymer and its retarding effect on cement hydration, it is still higher than the control mixture. AA-AM copolymer fills the pores in the cement matrix, as presented in Fig. 13, which densifies the inner structure. Furthermore, the improved ITZ between Field's metal and cement matrix discussed in Section 3.5 is conducive to increasing the compressive strength.

Flexural strength in all types of samples is higher than the control mixture regardless of curing days, as illustrated in Fig. 11(b). Adding 5% of Field's metal increases the flexural strength slightly (~10%), resulting from the melting Field's metal can fill microcracks in the cement matrix, which is in agreement with [31]. It is noteworthy that adding 3% AA-AM copolymer increases the flexural strength by 107.8% at 28 days compared with the control mixture, and the 28-day flexural strength is further increased by 174.2% with the coupling effect of Field's metal and AA-AM copolymer. The significant increase in flexural strength for A3 is attributed to the formation of an interpenetrating polymer-cement network via *in situ* polymerization of AA and AM and the filling effect of the AA-AM copolymer. For samples modified with Field's metal and AA-AM copolymer, AA-AM copolymer enhances the ITZ between Field's metal and cement matrix (Fig. 7) and connects them by the polymer chain to form a strong composite. During heating curing, the unhydrated cement particles in A3F5 are stimulated to rehydrate, generating more CH, as shown in Fig. 5(b). This increased CH content indicates that the hydration degree is promoted under heating, contributing to the sharp increase in flexural strength. *In situ* polymerization of AA and AM during

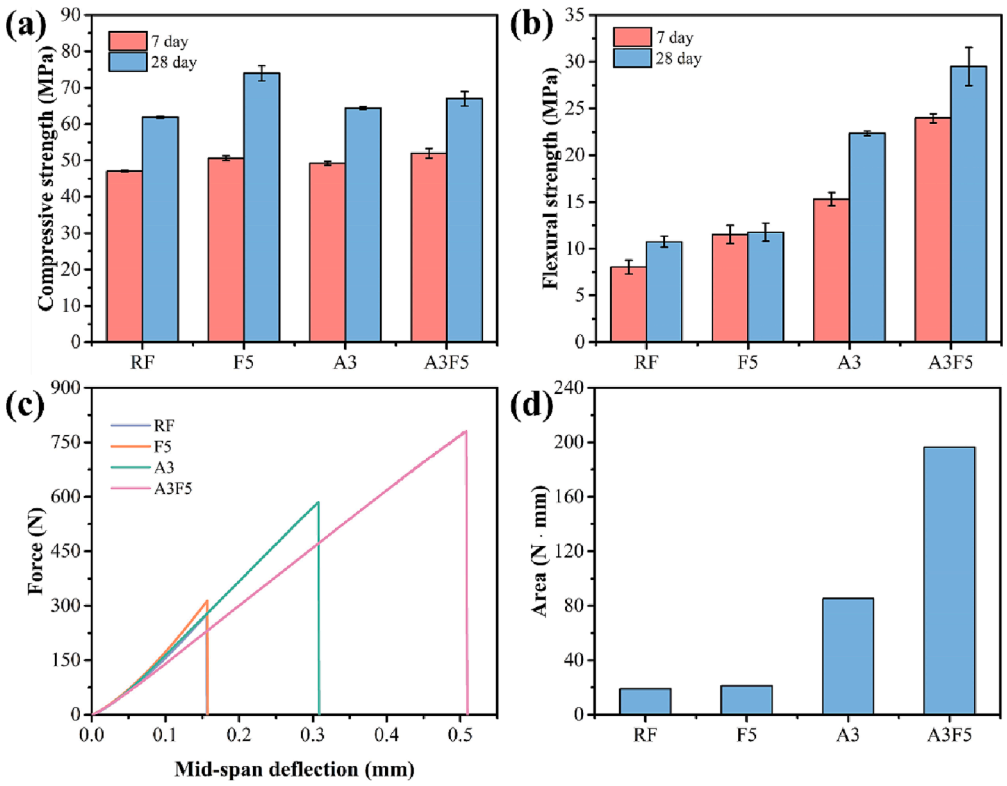

Fig. 11. Mechanical strength of the cement composites. (a) Compressive strength; (b) Flexural strength; (c) Force-deflection curves; (d) Area below the force–deflection curves.

cement hydration weaves a polymer-cement network with stiffness and softness, and while Field's metal fills the microcracks of the cement matrix via melting, both of which cooperates and complements with each other, leading to a sharp improvement in the flexural strength. In addition, Field's metal and AA-AM copolymer drastically decrease the peak temperature of cement hydration (Fig. 4), reducing the crack caused by thermal stress, which enhances flexural strength.

From the force–deflection curve (Fig. 11(c)), adding Field's metal increases the force that cement composites can bear, whereas Field's metal-modified samples show the same deflection as the reference mixture, suggesting that Field's metal has limited influence on the toughness of cement matrix. Conversely, samples with AA-AM copolymer or Field's metal and AA-AM copolymer exhibit a higher force and longer mid-span deflection, among which those with AA-AM copolymer and Field's metal have a deflection of more than 0.5 mm. This increased force and deflection manifest that the toughness and crack resistance of the cement composites are enhanced. The toughness of cementitious materials can be evaluated from the area below their force–deflection curves. As shown in Fig. 11(d), the area of F5 is slightly higher than the reference mixture, which is in line with the flexural strength. For A3F5, the area is sharply increased to 196 N·mm, roughly 9.3 times larger than the control sample, signifying that this cement composite absorbs much more energy and its toughness is strengthened. The strengthened toughness is because the polymer network crosslinks with hydration products and endows flexibility to the brittle cement matrix. The melting Field's metal fills the microcracks, decreasing the defect in the matrix, which further increases the toughness.

A comparison of compressive and flexural strength for cementitious materials enhanced by different materials is illustrated in Fig. 12. The value that gets closer to the red line indicates that this material possesses high compressive and flexural strength. It is apparent that most materials are below the red line, suggesting they own high compressive strength but relatively low flexural strength. Fibers can significantly improve mechanical strength via the bonding with cement matrix,

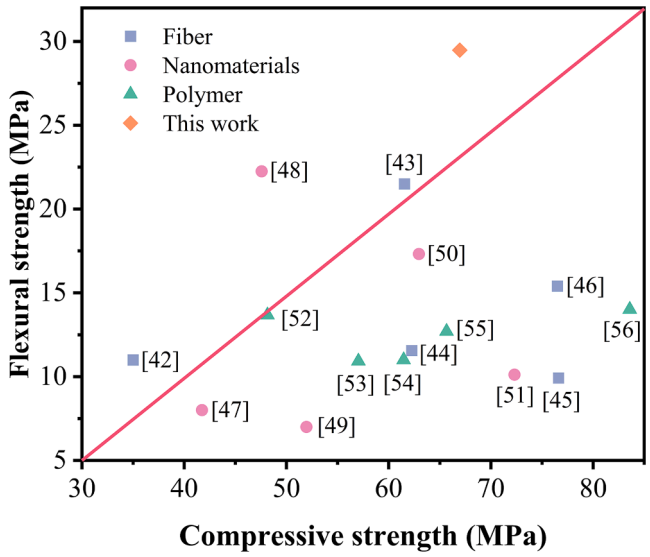

Fig. 12. Comparison of compressive and flexural strength for cementitious materials enhanced by different materials. Fibers [48–52]; Nanomaterials [53–57]; Polymers [6,58–61].

which belongs to physical enhancement. Our work realizes the significant increase in flexural strength by enhancing the toughness of the cement matrix and gains high compressive strength simultaneously, manifesting that the coupling effect of Field's metal and *in situ* polymerization of monomers is more effective than traditional polymer and nanomaterials in improving the mechanical strength, especially for flexural strength. It is believed that combing our method with fibers can achieve multi-scale enhancement for cement-based materials.

3.7. Pore structure

Fig. 13 depicts the pore structure of the cement composites after curing for 28 days. The pore size is shifted toward the finer area with the addition of the AA-AM copolymer, accompanied by a decrease in the cumulative pore volume. This refined pore structure is mainly due to the filling effect of the AA-AM copolymer formed during cement hydration, conducing to enhance the mechanical strength of the cement composites. However, only adding Field's metal shifts the pore size to the coarse area slightly without influencing the cumulative pore volume, which probably is because the flow of melting Field's metal leaves a cavity on its original site. The cumulative pore volume against pore size diameter is presented in Fig. 13(b). Samples modified by AA-AM copolymer and Field's metal show a slightly higher for pores less than 50 nm compared to the reference mixture, which agrees with the study by Ballester et al. [62]. The fast hydration remains the cement hydrates around the cement particles under high temperatures and leaves an open interstitial space [63], which increases the finer pores.

The pores below 10 nm, 10–50 nm, 50–1000 nm, and above 1000 nm are assigned to gel pores, mesopores, capillary pores, and large pores, respectively. Adding Field's metal and AA-AM copolymer (A3F5) decreases the gel pores by 25.4%, whereas the mesopores increase with the addition of Field's metal or AA-AM copolymer (Fig. 13(c)). Pores larger than 50 nm were regarded as harmful pores [64], which have an adverse impact on the durability of cementitious materials. The harmful pores are reduced for samples with Field's metal or AA-AM copolymer due to their filling effect that transforms these pores into mesopores. The densified pore structure is conducive to improving the mechanical strength and durability of the cement composites.

4. Conclusions

This work mainly developed a mechanically strong cement composite by combining Field's metal with *in situ* polymerization of AA and AM. We investigated the effects of Field's metal and AA-AM copolymer on fluidity, hydration temperature, microstructure, and mechanical strength of cement composites. Based on the results, some conclusions can be drawn.

1. Adding Field's metal decreases the fluidity of the cement composite, while AA-AM copolymer increases the fluidity by absorption on the surface of the cement particles.
2. The peak temperature of cement hydration is dramatically reduced in the presence of Field's metal due to its low melting point, which decreases the risk of thermal crack. Coupling the Field's metal and AA-AM copolymer retards the cement hydration and reduces the peak temperature further.
3. Field's metal has limited influence on the amount of CH, whereas AA-AM copolymer sharply decreases its content. Heating curing promotes the hydration of unreacted cement particles in samples with Field's metal and AA-AM copolymer.
4. AA-AM copolymer densifies the ITZ between Field's metal and cement matrix and connects them, resulting in the enhancement of mechanical strength. The *in situ* polymerized polymer network provides flexibility to the cement hydrates and improves the toughness

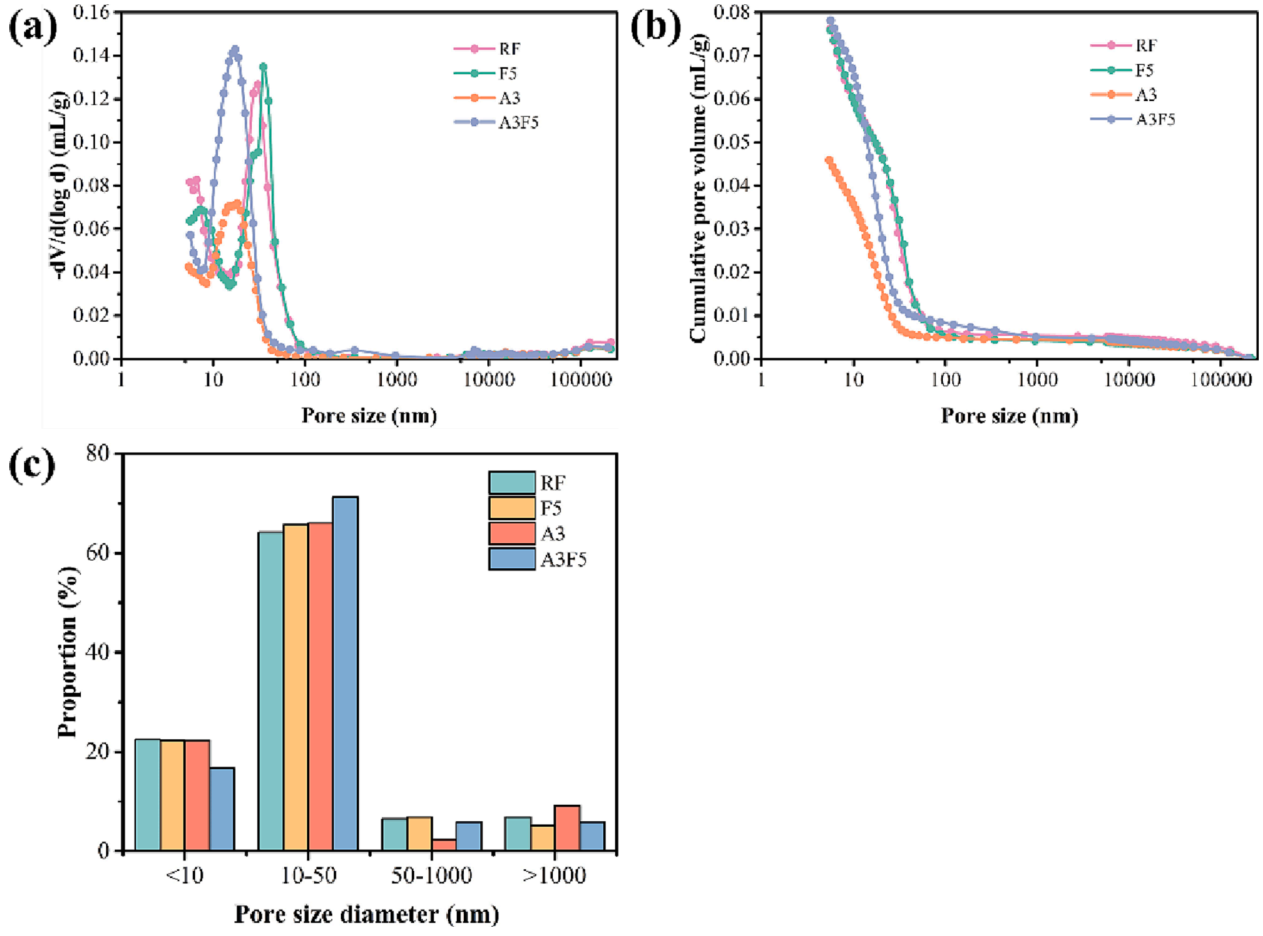

Fig. 13. The pore structure of the cementitious materials at 28 days. (a) Cumulative pore volume; (b) Pore size distribution; (c) The proportion of pores with different diameters.

of the cement composite. The flow of the Field's metal is achieved by heating curing, which fills the microcracks.
5. The mechanical strength is increased with the addition of Field's metal or AA-AM copolymer, among which A3F5 exhibits the highest flexural strength, approximately 174.2 % higher than the reference mixture, and maintains high compressive strength.
6. The pore volume is decreased for samples with Field's metal and AA-AM copolymer. This phenomenon is more pronounced in AA-AM copolymer-modified cement composites, arising from the filling effect of AA-AM copolymer.

This study offers a new way to improve mechanical strength, from inhibiting the thermal crack to reducing the brittleness of the cement matrix. It is necessary to pay attention to the retarding effect of AA-AM copolymer on cement hydration for future applications. Based on the low melting point of Field's metal, this material can be used as a new phase change material (PCM), which not only decreases the indoor temperature variations but also avoids the leakage of traditional PCMs and improves the mechanical strength of the material.

CRediT authorship contribution statement

Qing Liu: Data curation, Formal analysis. **Xing Ming:** Data curation, Formal analysis. **Jianyu Xu:** Resources, Visualization. **Dongshuai Hou:** Visualization. **Guoxing Sun:** Funding acquisition, Validation, Writing – review & editing. **Zongjin Li:** Conceptualization, Funding acquisition, Supervision, Writing – review & editing. **Guoqing Geng:** Funding acquisition, Validation, Writing – review & editing.

Declaration of Competing Interest

The authors declare that they have no known competing financial interests or personal relationships that could have appeared to influence the work reported in this paper.

Data availability

Data will be made available on request.

Acknowledgements

This work was funded by National Natural Science Foundation of China, Excellent Young Scientists Fund (HK&Macau) (File no. 5212290021); Shenzhen-Hong Kong-Macao science and technology plan (c) (File no. SGDX2020110309360); by The Science and Technology Development Fund, Macau SAR (File no. 0138/2020/A3).

References

[1] J. Hong, G.Q. Shen, Y. Feng, W.-T. Lau, C. Mao, Greenhouse gas emissions during the construction phase of a building: A case study in China, J. Clean. Prod. 103 (2015) 249–259.
[2] Z. Ma, J. Shen, C. Wang, H. Wu, Characterization of sustainable mortar containing high-quality recycled manufactured sand crushed from recycled coarse aggregate, Cem. Concr. Compos. 132 (2022), 104629.
[3] M. Liu, H. Wu, P. Yao, C. Wang, Z. Ma, Microstructure and macro properties of sustainable alkali-activated fly ash mortar with various construction waste fines as binder replacement up to 100%, Cem. Concr. Compos. 134 (2022), 104733.
[4] B. Liu, J. Shi, M. Sun, Z. He, H. Xu, J. Tan, Mechanical and permeability properties of polymer-modified concrete using hydrophobic agent, J. Build. Eng. 31 (2020), 101337.
[5] R. Wetzel, O. Eckardt, P. Biehl, D. Brauer, F. Schacher, Effect of poly (acrylic acid) architecture on setting and mechanical properties of glass ionomer cements, Dent. Mater. 36 (3) (2020) 377–386.
[6] U. Rai, R. Singh, Effect of polyacrylamide on the different properties of cement and mortar, Mater. Sci. Eng. A 392 (1–2) (2005) 42–50.
[7] Z. Sun, Q. Xu, Micromechanical analysis of polyacrylamide-modified concrete for improving strengths, Mater. Sci. Eng. A 490 (1–2) (2008) 181–192.
[8] R. Wang, R. Lackner, P.M. Wang, Effect of styrene–butadiene rubber latex on mechanical properties of cementitious materials highlighted by means of nanoindentation, Strain 47 (2) (2011) 117–126.
[9] A.C. Bhogayata, N.K. Arora, Workability, strength, and durability of concrete containing recycled plastic fibers and styrene-butadiene rubber latex, Constr. Build. Mater. 180 (2018) 382–395.
[10] S. Zhong, Z. Chen, Properties of latex blends and its modified cement mortars, Cem. Concr. Res. 32 (10) (2002) 1515–1524.
[11] Z. Yang, X. Shi, A.T. Creighton, M.M. Peterson, Effect of styrene–butadiene rubber latex on the chloride permeability and microstructure of Portland cement mortar, Constr. Build. Mater. 23 (6) (2009) 2283–2290.
[12] K.-R. Wu, D. Zhang, J.-M. Song, Properties of polymer-modified cement mortar using pre-enveloping method, Cem. Concr. Res. 32 (3) (2002) 425–429.
[13] H. Zhang, R. Zhou, S. Liu, Y. Zhu, S. Wang, J. Wang, X. Guan, Enhanced toughness of ultra-fine sulphoaluminate cement-based hybrid grouting materials by incorporating in-situ polymerization of acrylamide, Constr. Build. Mater. 292 (2021), 123421.
[14] R. Liang, Q. Liu, D. Hou, Z. Li, G. Sun, Flexural strength enhancement of cement paste through monomer incorporation and in situ bond formation, Cem. Concr. Res. 152 (2022), 106675.
[15] Q. Liu, W. Liu, Z. Li, S. Guo, G. Sun, Ultra-lightweight cement composites with excellent flexural strength, thermal insulation and water resistance achieved by establishing interpenetrating network, Constr. Build. Mater. 250 (2020), 118923.
[16] B. Yin, X. Hua, D. Qi, P. Wang, G. Qiao, F. Fan, X. Hua, X. Wang, D. Hou, Performance cement-based composite obtained by in-situ growth of organic–inorganic frameworks during the cement hydration, Constr. Build. Mater. 336 (2022), 127533.
[17] C. Xu, Y. Dai, Y. Peng, J. Wang, Z. Zhang, Q. Gui, Q. Zeng, Multi-scale structure of in-situ polymerized cementitious composites with improved flowability, strength, deformability and anti-permeability, Compos. B. Eng. 245 (2022), 110222.
[18] B. Chen, G. Qiao, D. Hou, M. Wang, Z. Li, Cement-based material modified by in-situ polymerization: From experiments to molecular dynamics investigation, Compos. B Eng. 194 (2020), 108036.
[19] B. Myszka, K. Hurle, K. Zheng, S.E. Wolf, A.R. Boccaccini, Mechanical improvement of calcium carbonate cements by in situ HEMA polymerization during hardening, J. Mater. Chem. B 7 (21) (2019) 3403–3411.
[20] S.-W. Son, J.H. Yeon, Mechanical properties of acrylic polymer concrete containing methacrylic acid as an additive, Constr. Build. Mater. 37 (2012) 669–679.
[21] T.V. Neumann, M.D. Dickey, Liquid metal direct write and 3D printing: a review, Adv. Mater. Technol. 5 (9) (2020) 2000070.
[22] S.E. Byeon, H. Kang, H.J. Yoon, Toward Printed Molecular Electronics: Direct Printing of Liquid Metal Microelectrode on Self-Assembled Monolayers, Adv. Electron. Mater. 7 (2) (2021) 2000829.
[23] S. Chen, J. Liu, Pervasive liquid metal printed electronics: From concept incubation to industry, IScience 24 (1) (2021), 102026.
[24] S. Zhang, Y. Liu, Q. Fan, C. Zhang, T. Zhou, K. Kalantar-Zadeh, Z. Guo, Liquid metal batteries for future energy storage, Energy Environ. Sci. 14 (8) (2021) 4177–4202.
[25] S. Park, H.J. Yoon, New Approach for large-area thermoelectric junctions with a liquid eutectic gallium–indium electrode, Nano Lett. 18 (12) (2018) 7715–7718.
[26] K. Zuraiqi, A. Zavabeti, F.-M. Allioux, J. Tang, C.K. Nguyen, P. Tafazolymotie, M. Mayyas, A.V. Ramarao, M. Spencer, K. Shah, C.F. McConville, K. Kalantar-Zadeh, K. Chiang, T. Daeneke, Liquid metals in catalysis for energy applications, Joule 4 (11) (2020) 2290–2321.
[27] K. Zuraiqi, C.J. Parker, A. Zavabeti, A.J. Christofferson, S. Maniam, C. F. McConville, K. Chiang, T. Daeneke, Field's Metal Nanodroplets for Creating Phase-Change Materials, ACS Appl. Nano Mater. 5 (5) (2022) 5952–5958.
[28] K.M. Nemati, P.J. Monteiro, A new method to observe three-dimensional fractures in concrete using liquid metal porosimetry technique, Cem. Concr. Res. 27 (9) (1997) 1333–1341.
[29] Y. Liu, S.J. Chen, K. Sagoe-Crentsil, W. Duan, Evolution of tricalcium silicate (C3S) hydration based on image analysis of microstructural observations obtained via Field's metal intrusion, Mater. Charact. 181 (2021), 111457.
[30] J. Kaufmann, Pore space analysis of cement-based materials by combined Nitrogen sorption–Wood's metal impregnation and multi-cycle mercury intrusion, Cem. Concr. Compos. 32 (7) (2010) 514–522.
[31] J. Xu, Q. Liu, H. Guo, M. Wang, Z. Li, G. Sun, Low melting point alloy modified cement paste with enhanced flexural strength, lower hydration temperature, and improved electrical properties, Compos. B Eng. 232 (2022), 109628.
[32] B. Xu, H. Ma, Z. Li, Influence of magnesia-to-phosphate molar ratio on microstructures, mechanical properties and thermal conductivity of magnesium potassium phosphate cement paste with large water-to-solid ratio, Cem. Concr. Res. 68 (2015) 1–9.
[33] Q. Liu, Z. Lu, J. Xu, Z. Li, G. Sun, Insight into the in situ copolymerization of monomers on cement hydration and the mechanical performance of cement paste, J. Sustain. Cem.-Based Mater. (2022) 1–15.
[34] Q. Liu, Z. Lu, X. Hu, B. Chen, Z. Li, R. Liang, G. Sun, A mechanical strong polymer-cement composite fabricated by in situ polymerization within the cement matrix, J. Build. Eng. 42 (2021), 103048.
[35] A.M. Betioli, P.J.P. Gleize, V.M. John, R.G. Pileggi, Effect of EVA on the fresh properties of cement paste, Cem. Concr. Compos. 34 (2) (2012) 255–260.
[36] J. Yan, M.H. Malakooti, Z. Lu, Z. Wang, N. Kazem, C. Pan, M.R. Bockstaller, C. Majidi, K. Matyjaszewski, Solution processable liquid metal nanodroplets by surface-initiated atom transfer radical polymerization, Nat. Nanotechnol. 14 (7) (2019) 684–690.
[37] N. Mehra, L. Mu, J. Zhu, Developing heat conduction pathways through short polymer chains in a hydrogen bonded polymer system, Compos. Sci. Technol. 148 (2017) 97–105.

[38] Z. Lu, X. Kong, C. Zhang, Y. Cai, Effect of highly carboxylated colloidal polymers on cement hydration and interactions with calcium ions, Cem. Concr. Res. 113 (2018) 140–153.
[39] T. He, C. Shi, G. Li, X. Song, Effects of superplasticizers on the carbonation resistance of C3S and C3A hydration products, Constr. Build. Mater. 36 (2012) 954–959.
[40] Q. Lv, Y. Shen, Y. Qiu, M. Wu, L. Wang, Poly (acrylic acid)/poly (acrylamide) hydrogel adsorbent for removing methylene blue, J. Appl. Polym. Sci. 137 (43) (2020) 49322.
[41] S. Shirani, A. Cuesta, A. Morales-Cantero, G. Angeles, M.P. Olbinado, M.A. Aranda, Influence of curing temperature on belite cement hydration: A comparative study with Portland cement, Cem. Concr. Res. 147 (2021), 106499.
[42] E. Gallucci, X. Zhang, K.L. Scrivener, Effect of temperature on the microstructure of calcium silicate hydrate (CSH), Cem. Concr. Res. 53 (2013) 185–195.
[43] S. Bahafid, S. Ghabezloo, M. Duc, P. Faure, J. Sulem, Effect of the hydration temperature on the microstructure of Class G cement: CSH composition and density, Cem. Concr. Res. 95 (2017) 270–281.
[44] Y. Zhang, X. Kong, Correlations of the dispersing capability of NSF and PCE types of superplasticizer and their impacts on cement hydration with the adsorption in fresh cement pastes, Cem. Concr. Res. 69 (2015) 1–9.
[45] E. Knapen, D. Van Gemert, Microstructural analysis of paste and interfacial transition zone in cement mortars modified with water-soluble polymers, Key Eng. Mater., Trans Tech Publ, 2011, pp. 21–28.
[46] R. Yang, J.H. Sharp, Hydration characteristics of Portland cement after heat curing: I, Degree of hydration of the anhydrous cement phases, J. Am. Ceram. Soc. 84 (3) (2001) 608–614.
[47] B. Lothenbach, F. Winnefeld, C. Alder, E. Wieland, P. Lunk, Effect of temperature on the pore solution, microstructure and hydration products of Portland cement pastes, Cem. Concr. Res. 37 (4) (2007) 483–491.
[48] J. Donnini, T. Bellezze, V. Corinaldesi, Mechanical, electrical and self-sensing properties of cementitious mortars containing short carbon fibers, J. Build. Eng. 20 (2018) 8–14.
[49] Z.-S. Chen, X. Zhou, X. Wang, P. Guo, Mechanical behavior of multilayer GO carbon-fiber cement composites, Constr. Build. Mater. 159 (2018) 205–212.
[50] C. Pei, T. Ueda, J. Zhu, Investigation of the effectiveness of graphene/polyvinyl alcohol on the mechanical and electrical properties of cement composites, Mater. Struct. 53 (2020) 1–15.
[51] C. Li, A. Zhou, J. Zeng, Z. Liu, Z. Zhang, Influence of MFPSA on mechanical and hydrophobic behaviour of fiber cement products, Constr. Build. Mater. 223 (2019) 1016–1029.
[52] W. Jiang, X. Li, Y. Lv, M. Zhou, Z. Liu, Z. Ren, Z. Yu, Cement-based materials containing graphene oxide and polyvinyl alcohol fiber: mechanical properties, durability, and microstructure, Nanomaterials 8 (9) (2018) 638.
[53] M. Stefanidou, I. Papayianni, Influence of nano-SiO2 on the Portland cement pastes, Compos. B. Eng. 43 (6) (2012) 2706–2710.
[54] W. Li, X. Li, S.J. Chen, G. Long, Y.M. Liu, W.H. Duan, Effects of nanoalumina and graphene oxide on early-age hydration and mechanical properties of cement paste, J. Mater. Civ. Eng. 29 (9) (2017) 04017087.
[55] Z. Pan, L. He, L. Qiu, A.H. Korayem, G. Li, J.W. Zhu, F. Collins, D. Li, W.H. Duan, M.C. Wang, Mechanical properties and microstructure of a graphene oxide–cement composite, Cem. Concr. Compos. 58 (2015) 140–147.
[56] L. Yang, Z. Jia, Y. Zhang, J. Dai, Effects of nano-TiO2 on strength, shrinkage and microstructure of alkali activated slag pastes, Cem. Concr. Compos. 57 (2015) 1–7.
[57] S. Musso, J.-M. Tulliani, G. Ferro, A. Tagliaferro, Influence of carbon nanotubes structure on the mechanical behavior of cement composites, Compos. Sci. Technol. 69 (11–12) (2009) 1985–1990.
[58] X. Li, R. Liu, S. Li, C. Zhang, J. Li, B. Cheng, Y. Liu, C. Ma, J. Yan, Effect of SBR and XSBRL on water demand, mechanical strength and microstructure of cement paste, Constr. Build. Mater. 332 (2022), 127309.
[59] S.-Y. Guo, X. Zhang, J.-Z. Chen, B. Mou, H.-S. Shang, P. Wang, L. Zhang, J. Ren, Mechanical and interface bonding properties of epoxy resin reinforced Portland cement repairing mortar, Constr. Build. Mater. 264 (2020), 120715.
[60] C. Shi, X. Zou, P. Wang, Influences of EVA and methylcellulose on mechanical properties of Portland cement-calcium aluminate cement-gypsum ternary repair mortar, Constr. Build. Mater. 241 (2020), 118035.
[61] Y. He, L. Mo, Z. Mao, F. Huang, Z. Han, Influence of Polyvinyl Alcohol Powder on the Mechanical Performance and Volume Stability of Sulfoaluminate-Portland Cement Composite, Crystals 11 (6) (2021) 692.
[62] P. Ballester, A. Hidalgo, I. Mármol, J. Morales, L. Sánchez, Effect of brief heat-curing on microstructure and mechanical properties in fresh cement based mortars, Cem. Concr. Res. 39 (7) (2009) 573–579.
[63] A.A. Almusallam, Effect of environmental conditions on the properties of fresh and hardened concrete, Cem. Concr. Compos. 23 (4–5) (2001) 353–361.
[64] Q. Wang, S. Li, S. Pan, X. Cui, D.J. Corr, S.P. Shah, Effect of graphene oxide on the hydration and microstructure of fly ash-cement system, Constr. Build. Mater. 198 (2019) 106–119.